AIP | Review of Scientific Instruments

High performance electronic device for the measurement of the inverse spin Hall effect

Javier E. Gómez, Matías Guillén, Alejandro Butera, and Neil P. Albaugh

Citation: Review of Scientific Instruments **87**, 024705 (2016); doi: 10.1063/1.4942178
View online: http://dx.doi.org/10.1063/1.4942178
View Table of Contents: http://scitation.aip.org/content/aip/journal/rsi/87/2?ver=pdfcov
Published by the AIP Publishing

High performance electronic device for the measurement of the inverse spin Hall effect

Javier E. Gómez,[1,a)] Matías Guillén,[1] Alejandro Butera,[2,a)] and Neil P. Albaugh[3]
[1]*Centro Atómico Bariloche (CNEA) and Conicet, 8400 Bariloche, Río Negro, Argentina*
[2]*Centro Atómico Bariloche (CNEA), Instituto Balseiro (U. N. Cuyo), and Conicet, 8400 Bariloche, Río Negro, Argentina*
[3]*Diamond Bell Technology LLC, Tucson, Arizona 85736, USA*

(Received 4 November 2015; accepted 4 February 2016; published online 23 February 2016)

We have developed a high performance analog electronic device that can be used for the measurement of the inverse spin Hall effect (ISHE) as a function of the applied magnetic field. The electronic circuit is based on the synchronous detection technique with a careful selection of the active components in order to optimize the response in this application. The electronic accessory was adapted for the simultaneous measurement of the ISHE signal and the microwave absorption in an electron spin resonance spectrometer and tested with a bilayer sample of 5 nm of permalloy ($Ni_{80}Fe_{20}$) and 5 nm of tantalum. The response of the electronic device was characterized as a function of the microwave power, the amplitude and frequency of the modulation signal, and the relative phase between signal and reference. This last characterization reveals a simple method to put in phase the signal with the reference. The maximum signal to noise ratio was achieved for a modulation frequency between 6 and 12 kHz, for the largest possible values of field modulation amplitude and microwave power. © *2016 AIP Publishing LLC.* [http://dx.doi.org/10.1063/1.4942178]

I. INTRODUCTION

Synchronous detection is a commonly and widely used technique to measure low level voltage signals buried with unwanted noise. In general, a reference ac signal is used to modulate a slowly varying signal in order to shift the response to relatively high frequencies, where the undesired $1/f$ noise is significantly smaller. The ac response is the input signal to an electronic device which is used to amplify, demodulate, and filter this signal and generates an output dc signal with a greatly improved signal to noise ratio. This technique works synchronously with the reference and the input signals, and the amplitude and relative phase between both signals can be measured while an experiment is carried on. As the technique is sensitive to the relative phase, it is also known as phase sensitive detection (PSD) or simply as a lock-in amplifier (LIA).

On the other hand, a great effort has been lately devoted to the manipulation of the electron spin in order to incorporate this degree of freedom in electronic devices.[1,2] The research in spin electronics (or spintronics) led to the discovery of the ability of some engineered systems to continuously inject angular momentum in the form of a pure spin current, which has opened a new window to experimentally study and understand novel spin transport mechanisms, at least from the point of view of the basic research.[2,3] This phenomenon, known as *spin pumping,* can be observed when a ferromagnetic (FM) thin film, which is driven to its magnetic resonance condition, is put in close contact with non-magnetic (NM) metal film. In such a bilayer system, the conduction electrons of the NM mediate the relaxation of the excited ferromagnet by means of the injection of a pure spin current moving in a direction perpendicular to the interface and polarized parallel to the magnetization. This spin current can be detected by measuring a voltage between the ends of the sample. The voltage is originated by the inverse spin Hall effect (ISHE), a phenomenon that converts the spin current into a charge accumulation at the edges of the NM metal.[2,4,5] How efficiently the spin current is injected into the NM and subsequently converted into a charge accumulation strongly depends on the characteristics of the FM/NM interface and the nature of the NM metal. For such a reason a proper choice of the bilayer constituents is crucial to maximize the inverse spin Hall effect.

The ferromagnetic layer can be driven to resonance by different techniques, but either an Electron Spin Resonance (ESR) spectrometer or a Vector Network Analyzer (VNA) are the preferred instruments used for this purpose.

In this article, we present an electronic accessory based on the synchronous detection technique that can be added to these instruments in order to detect the inverse spin Hall effect. Particularly, the developed electronic device has been implemented and tested in an ESR spectrometer taking advantage of the magnetic field modulation that this equipment uses, but can be adapted to other instruments by properly modulating the signal to be measured.

II. ESR TECHNIQUES AND THE INVERSE SPIN HALL EFFECT

Electron spin resonance is a generic denomination for all magnetic resonance processes that involve the spin of the electrons. A finer classification can be done by considering the magnetic order of the material. Despite that the ESR phenomenon is essentially the same, the mathematical treatment is

[a)]Also at INN - Instituto de Nanociencia y Nanotecnología.

usually different. This is the underlying reason for the classification depending on the magnetic order of the studied material: paramagnetic resonance (EPR), ferromagnetic resonance (FMR), and antiferromagnetic resonance (AFMR).

We start with a brief description of the FMR theory, the spectrometer and the basis of the inverse spin Hall effect phenomenon in a bilayer system.

A. Brief introduction to FMR

Ferromagnetic resonance is a spectroscopic technique largely used to determine different quantities of the sample under study such as the anisotropy fields, the damping parameter (α), the g-factor, among other properties.[6] In a classical description, the technique describes the fact that when an external magnetic field is applied, a torque is exerted on the magnetization. The dynamical response obeys the phenomenological Landau-Lifshitz-Gilbert equation (Eq. (1)),

$$\frac{d\mathbf{M}}{dt} = -\gamma \mathbf{M} \times \mathbf{H} + \frac{\alpha}{M} \mathbf{M} \times \frac{d\mathbf{M}}{dt}, \tag{1}$$

where $\mathbf{M}$ is the magnetization, $\mathbf{H}$ is the total magnetic field that includes the external, anisotropy, and eventually exchange fields, and $\gamma = g\mu_B/\hbar$ is the gyromagnetic ratio. Briefly, the torque exerted on the magnetization drives its precession with an angular frequency ω governed by the first term of the Eq. (1). In real samples, the precession is quickly suppressed by the damping mechanisms that tend to align the magnetization parallel to $\mathbf{H}$ in order to minimize the energy. The damping mechanism is mathematically taken into account by the second term of the same equation. In the experimental setup, a perturbative time-dependent magnetic field of frequency $\omega_{\mu w}$ is applied in a direction perpendicular to a slowly varying external field. This magnetic field is varied in order to tune the precession frequency with the applied perturbative field frequency ($\omega = \omega_{\mu w}$). In such a condition, the sample absorbs energy from the microwave field, and is said to be in a magnetic resonance condition. For typical laboratory magnetic fields ($0\text{-}2 \times 10^4$ Oe), the precession frequency is usually in the range of 1-40 GHz.

In practice, a small amplitude modulation ($\mathbf{H}_{mod}$) of the quasi-static external magnetic field is added in order to increase the signal to noise ratio by removing contributing components with frequencies not close to the modulating frequency. Modulation is achieved by placing on the two outer sides of the resonant cavity, along the axis of the external magnetic field. The modulation frequency is known as the carrier frequency or simply as we mentioned before, the reference. The modulation frequency is in the range of 1-100 kHz.

In the FMR spectroscopy, the microwave absorption as a function of H is ideally a Lorentzian line. When the external field amplitude is modulated, the output of the detected signal is approximately proportional to the slope of the absorption near the midpoint of the modulating field, provided that the amplitude of the modulation is small compared to the line width of the measured line, as sketched in Fig. 1. The sign of the slope determines the output polarity of the synchronous detector. As a consequence, the output is the first derivative of the absorption signal as depicted in the inset of Fig. 1.

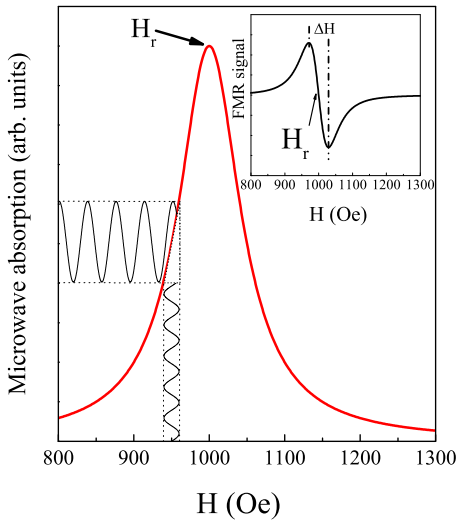

FIG. 1. Representation of the field modulation technique. While the external $\mathbf{H}$ field is slowly swept through the resonance, an additional magnetic field of relatively small amplitude is applied for modulation. As a consequence of this field modulation, the output signal is the first derivative of the absorption curve, as shown in the inset. The resonance field and the line width are also indicated.

A diagram of the most important parts of the FMR spectrometer is shown in Fig. 2. A waveguide transports the microwave electromagnetic radiation to a resonant cavity inside which a stationary oscillating magnetic field ($\mathbf{h}_{\mu w}$—perturbative field) of frequency $\omega_{\mu w}$ is maximum at the center. At this position, the microwave electric field vanishes and is the ideal region to place the sample. Outside the cavity walls, two Helmholtz coils provide the modulation field. The reflected microwave power is detected and demodulated by a lock-in amplifier while the quasi-static magnetic field is slowly varied during the resonance. The external magnetic field is called quasi-static because it is changed much slower than the microwave frequency (GHz range) or the modulation field (kHz range). While the field $\mathbf{H}$ is varied, the resonance condition is reached at some magnetic field (the resonance field position, H_r) with a certain dispersion (the line width, ΔH) as shown in the inset of Fig. 1.

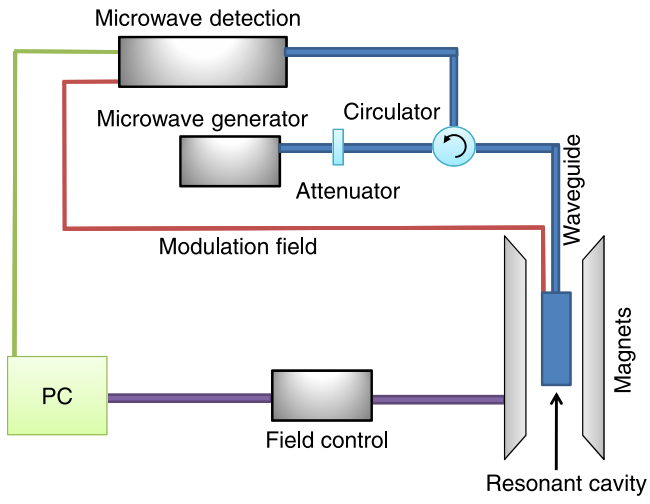

FIG. 2. Basic experimental setup of an electron spin resonance spectrometer.

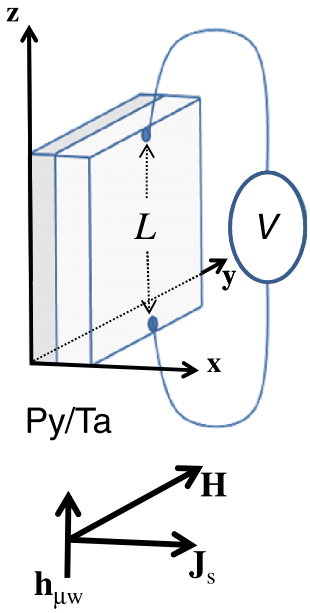

FIG. 3. Sketch of the geometrical array of the sample with respect to the microwave ($\mathbf{h}_{\mu w}$), external ($\mathbf{H}$) fields, and the injected spin current ($\mathbf{J}_s$). The ISHE voltage is measured transversally to the magnetization that lies parallel to $\mathbf{H}$. L corresponds to the distance between the electrodes where the voltage is measured.

In our experimental setup, the FMR spectra are acquired at room temperature using a commercial Bruker ESP 300 spectrometer operating at a microwave frequency of 9.4 GHz (X-band). The sample is placed in the center of a rectangular resonant cavity operating in the TE102 mode. The modulation frequency is usually 100 kHz with 5 Oe of amplitude and the maximum microwave power is ~200 mW. The sample plane was in all cases parallel to both the microwave excitation field and the external field as sketched in Fig. 3.

B. Inverse spin Hall effect

In a FMR experiment, the system under study absorbs energy from the microwave field. The line width of the measured signal provides information about the relaxation mechanisms of the magnetic excitation. As already stated, the second term of Eq. (1) considers phenomenologically the intrinsic part of this relaxation introducing the dimensionless Gilbert damping parameter, α, which is proportional to the line width.[7] The nature of relaxation mechanisms depend on the system under study, but despite the incomplete knowledge of the origin of α, it is well known that when a paramagnetic metal is put in close contact with a ferromagnetic thin film which is in resonance condition, an additional relaxation mechanism appears, mediated by the conduction electrons of the NM. The theory that describes the spin injection from a FM layer fulfilling the resonance condition into an adjacent NM layer is well established and numerous experimental results supporting these models can be found in the literature.[2,8–13] More precisely, a pure spin current appears as a consequence of an additional interfacial relaxation process, mediated by the conduction electrons of the normal metal. This additional relaxation through the interface is added to the intrinsic volume relaxation of the FM and then an increment in the line width (ΔH) of the bilayer system is expected when compared to a single FM layer which is not in contact with a NM. It is accepted that the voltage measured at the ends of the sample is originated by the injected spin current propagating in the $\hat{x}$ direction (perpendicular to the interface) and polarized along the magnetization direction $\hat{y}$ (the reference system is shown in Fig. 3). The dc pure spin current is converted into a charge current via the inverse spin Hall effect that deflects the electrons preferentially to one end of the sample. The edge of the sample where the charge accumulation takes place, depends on the sign of the deflection of the carriers, given by the sign of the spin Hall angle, Θ_{SH} (see Eq. (2))

$$\mathbf{J}_c = \Theta_{SH}\left(\frac{-2e}{\hbar}\right) J_s\,(\hat{x}\times\hat{y})\,, \tag{2}$$

where $\mathbf{J}_c$ is the charge current, J_s the spin current, $\hbar$ is the reduced Planck constant, and e is the electron charge. The unit vectors $\hat{x}$ and $\hat{y}$ are the propagation and polarization directions of the spin current, respectively.

Equation (2) indicates that the charge accumulation must be measured transversally to the magnetization axis, as depicted in Fig. 3.

It is generally observed that the injected spin current, and consequently the voltage measured between the edges of the bilayer, has the same line shape than the FMR absorption line.[13] Then a symmetric Lorentzian derivative is expected for the voltage (if phase sensitive detection is used). In practice, if the sample is not exactly in the middle of the cavity, additional effects coming from the non-zero electric field can contribute to the total measured voltage changing the line shape. We will not consider such effects here but they must be taken into account when a rigorous quantitative analysis is performed. A detailed explanation on how to consider these effects can be found in Ref. 8.

III. DESCRIPTION OF THE ELECTRONIC CIRCUITRY

The circuits developed in this work are depicted in Figs. 4 and 5 and are adaptations from circuits developed by Albaugh.

In Fig. 4, we distinguish the input stage where the voltage between the ends of the sample is monitored during the FMR experiment. This input stage consists of an ac coupled instrumentation amplifier (INA163, INA166, or INA217) suggested for low impedance source. Note that the metallic samples of few nanometer thickness used in this kind of experiments usually have a resistance of less than 1 kΩ (usually ~70-400 Ω). This makes the INA163 ideal for our purposes because its optimal performance is recommended and tested for a source impedance of 200 Ω. The ac coupling is performed by placing an integrator in the feedback to the reference of the INA163 in order to drive the dc output to 0 V. A FET OPA134 is put in a feedback loop for such a purpose. This operational amplifier is not in the signal path and should not affect the signal quality. The ac coupling is essential; if not placed, the dc component would completely mask the output signal.

The second stage is the synchronous demodulator. The OPA743 is a high slew rate operational amplifier that can work linearly almost up to the rail; as a consequence, the

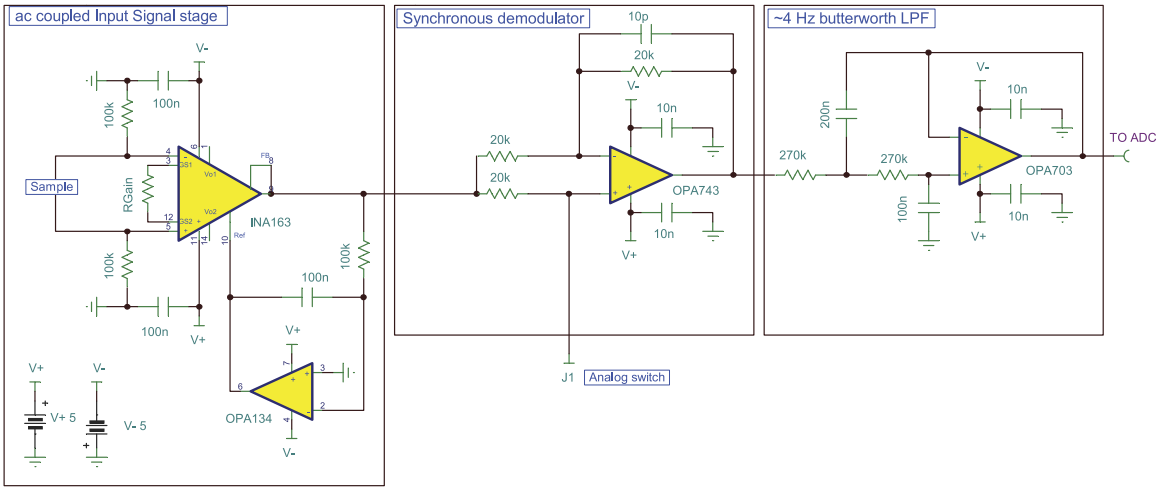

FIG. 4. Main circuit developed to measure the inverse spin Hall effect.

demodulator has a high dynamic range. Additionally its small slew rate asymmetry prevents offset error in the demodulation process. The aim of this circuit is to work as an unit gain amplifier, inverting or non-inverting depending on the state of a single voltage controlled analog switch connected at J1. When the switch is ON, it acts as a non-inverting unit gain amplifier and when it is OFF, as inverting. This property makes it possible to recover the previously modulated dc signal.[14]

For a proper demodulation, it is essential to synchronize the analog switch with the modulated signal. For such a reason the reference must be properly put in phase with the signal in order to synchronously activate the analog switch. This operation is performed by the phase shifter depicted in Fig. 5. Additionally a fast enough comparator (LM311 or LM111) is placed between the phase shifter and the analog switch. This comparator is placed because the reference is sinusoidal and to synchronize the input signal with the analog switch, a very sharp signal is necessary; then the comparator converts the sinusoidal into a square reference.

The measured inverse spin Hall voltage could be either negative or positive. For example, a sample rotation by 180°, the inversion of the external magnetic field, different bilayer structures or simply inverting the leads at the ends of the sample can result in an inversion of the sign of the ISHE voltage. For this reason, a dual power supply analog switch is necessary. We have used a TS12A4516 switch, as can be seen in Fig. 5.

Finally a second order butterworth low pass filter (LPF) is used to remove carrier artifacts and out-of-band noise. Random noise generated in the amplifier integrates to zero if a very long integration time (a very low cutoff frequency of the LPF) is used.

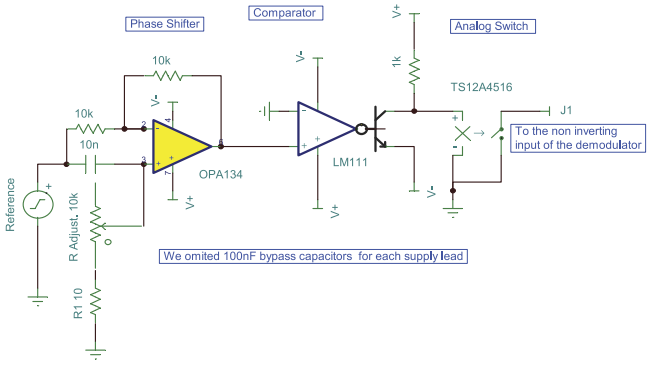

FIG. 5. Phase shifter and comparator to synchronously drive the analog switch connected at J1 of Fig. 4.

IV. EXPERIMENTAL RESULTS

In order to test the electronic device, a bilayer sample with a thickness of 5 nm of permalloy (Py) covered by 5 nm of tantalum (Ta) was grown by dc magnetron sputtering techniques. The growing method is fully described in Ref. 12. Two aluminium wires of 20 μm were attached at the ends of the sample with silver paste as shown in Fig. 3. Separation between the contacts was $L = 2$ mm. As already known, Ta has a negative spin Hall angle Θ_{SH} opposite to the positive value observed in platinum,[9] the most popular NM metal used for studying the ISHE phenomenon. We have used Ta because it produces a relatively thin line width in the absorption line (see Ref. 12).

Typical FMR and ISHE measurements are shown in Fig. 6 from which a resonance field position of 1194 Oe and a line width of 42 Oe can be determined. As expected, the line shape of both the measurements is almost coincident, although different physical magnitudes are measured in each case.

A. Reference, synchronizing, and calibration

Modern ESR equipment have an accessible voltage reference of the modulation field. In our system, we do not have a direct access to a reference and for this reason, we attached a small pick-up coil outside the resonant cavity in order to detect the disperse ac field generated by the modulation Helmholtz coils. We used a coil made up with a 100 μm diameter copper wire. The coil has an average diameter of 5 mm with around 500 turns. With this geometry, we measured an inductance of 0.68 mH. The signal captured by this coil is amplified and sent to the phase shifter sketched

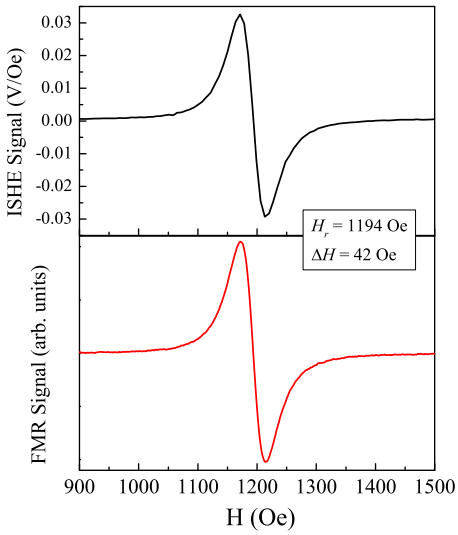

FIG. 6. Typical FMR and ISHE voltage measurements in a Py/Ta bilayer.

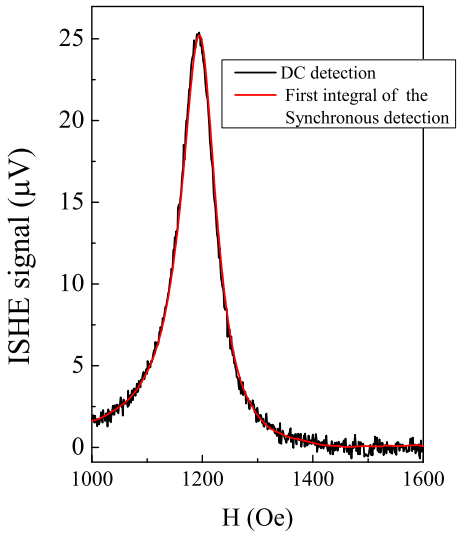

FIG. 8. DC detection performed with an instrumentation amplifier INA217 with a gain of 1000 and the first integral of the output signal. In our particular case, both curves superimpose if the signal (red curve) is multiplied by a factor 22.2.

in Fig. 5. The reference must be put in phase with the signal and this is obtained when the amplitude of the ISHE voltage is maximized.

It is worth mentioning that an offset in the measured output signal is normally present, which changes when the phase between the reference and the signal is adjusted. As shown in Fig. 7, the signal of the ISHE voltage is maximized when the offset is 0 V.

This last result can be explained by taking into account that the modulation field could induces an electromotive force (EMF) in the sample, leads and/or contacts. The induced EMF obeys Faraday's law and is then proportional to $\frac{\partial H_{mod}}{\partial t}$. If the time-dependent modulation field is proportional to $\sin(\Omega t)$, the induced EMF should be proportional to $\cos(\Omega t)$. On the other hand, the ISHE voltage is in phase with the modulation field and is then proportional to $\sin(\Omega t)$. This means that the induced EMF and the ISHE signal are 90° out of phase. In practice, we use this fact to synchronize the ISHE phase with the reference signal by driving the offset to 0 V. The results of this procedure are shown in Fig. 7 and the corresponding inset. The phase of the reference can be varied by changing the value of the potentiometer R adjust shown in Fig. 5. We have added a fixed resistance of 10 Ω in series to avoid the potentiometer reaching 0 Ω. If not placed, the phase shifter becomes unstable when the potentiometer is turned up to low values and the signal is lost.

Another point to be considered is the calibration of the gain of the device in order to properly estimate the absolute ISHE voltage. For quantitative results, this procedure is essential. To characterize our device, we compared the integral of the output signal with a dc detection performed with an instrumentation amplifier INA217 with a gain of 1000. As shown in Fig. 8, to fit both curves and read the values in μV, it is necessary to multiply the output signal by a factor 22.2.

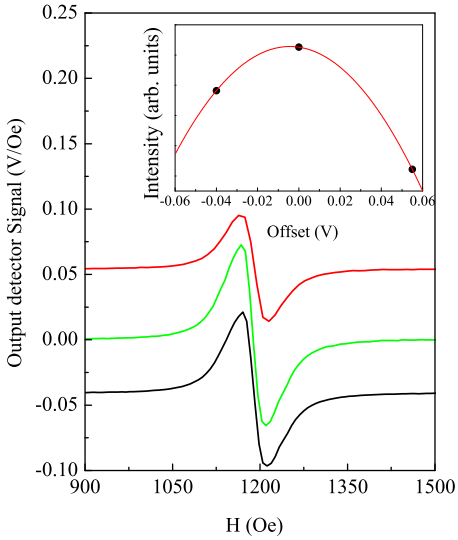

FIG. 7. ISHE voltage measured at different relative phases between the reference and the signal. The maximum ISHE signal is obtained when the offset is driven to 0 V.

B. Modulation amplitude

The field modulation amplitude is one of the important experimental parameters that can be changed in order to optimize the signal to noise ratio of the ISHE measurement. As in the case of the FMR detection technique depicted in Fig. 1, the ISHE voltage is measured in a similar way. In consequence, increasing the field modulation amplitude should result in a linear increment of the output signal. Fig. 9 shows the measured ISHE voltage for different modulation amplitudes in the range 5.6–28 Oe. The inset shows the expected linear evolution of the double integral of the line (the area under the absorption that can be interpreted as the intensity of the line) as a function of the modulation amplitude.

Some care must be taken for very large modulation amplitudes. If the modulation field is comparable to the line width, a deformation of the line shape occurs and a derivative of a Lorentzian line will no longer be observed. We also show in the inset of Fig. 9 the behavior of the line width

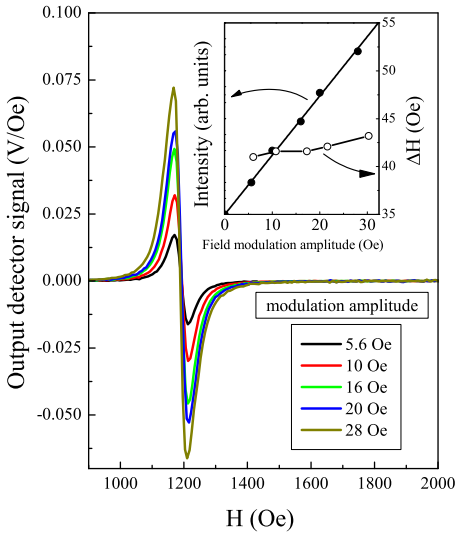

FIG. 9. ISHE voltage measured at different field modulation amplitudes. The inset shows the line intensity and the line width as a function of the modulation amplitude. (Modulation frequency = 1.56 kHz, microwave power = 200 mW.)

when the modulation frequency is changed. As expected, it remains almost unchanged with a very small increment when the modulation field increases, probably due to the above mentioned effect. It is generally accepted that for a rigorous quantitative interpretation of the line shape, the modulation field amplitude should not exceed 10% of the line width.

C. Power dependence

We have also studied the microwave power (P) dependence of the ISHE voltage. We show in Figs. 10(a) and 10(b) the signal obtained for different microwave powers and the corresponding first integral of the line shape. The inset shows that the maximum value of the first integral (which is a very good measure of the line intensity for low modulation fields) follows a linear behavior as a function of the microwave power.

As explained in the literature,[12] the linear dependence of the ISHE voltage as a function of P can be understood by inspection of the form of the dc spin current $J_s \propto \int_0^{\frac{2\pi}{\omega}} \left[m_x \frac{dm_z}{dt} - m_z \frac{dm_x}{dt} \right] dt$. As we are in the linear response regime ($\mathbf{m} = \underline{\chi}\mathbf{h}_{\mu w}$), each transversal component of the magnetization, $m_{i=x,z}$, contributes with a $h_{\mu w}$ factor, making $J_s \propto h_{\mu w}^2$ and hence, $V_{\mathrm{ISHE}} \propto h_{\mu w}^2$. As P is proportional to $h_{\mu w}^2$,[15] we can understand the linear behavior of the maximum ISHE voltage as a function of the microwave power, as shown in Fig. 10. The power dependence experiment was made in order to check that our electronic device works correctly in a relatively large range of input signals. We also show the line width behavior as a function of the microwave power. An almost constant value was found.

D. Modulation frequency

We have also checked the dependence of the output signal as a function of the field modulation frequency. As is already known, the modulation frequency should be different from interfering signals, like the power line frequency (50/60 Hz) or its harmonics. Also, by increasing the modulation frequency, we can move out of the $1/f$ noise region. Fig. 11 shows the dependence of the output signal for different modulation frequencies in the range 1-100 kHz. The inset shows a flat region of the spectra in order to observe qualitatively the noise level of the signal. As can be seen in the figure, a better performance is achieved when the frequency is between 6 and 12 kHz. It is actually surprising that the signal modulated at 100 kHz has the poorest signal to noise ratio when compared with lower frequency data. We think that this could be a consequence of the way we get the reference (by fixing a pick-up coil on the outside wall of the cavity). The coil was not impedance matched for different frequencies and may detect a poor reference signal at higher frequencies. As a consequence

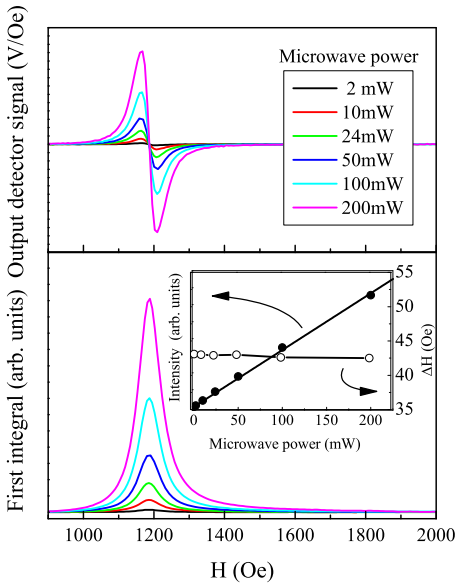

FIG. 10. ISHE voltage measured with different microwave powers. The inset shows the line intensity and line width as a function of the microwave power. (Modulation amplitude = 20 Oe, modulation frequency = 1.56 kHz.)

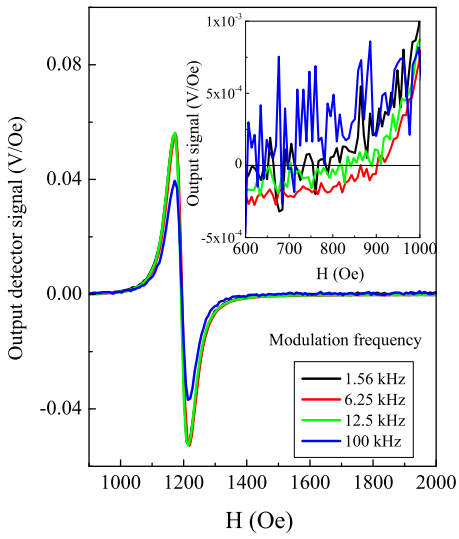

FIG. 11. Output signal measured at different field modulation frequencies. The inset shows a detail of a region with very small signal for the qualitative estimation of the signal to noise ratio.

of this, the comparator is driven by a poor and noisy reference degrading the overall performance of the detector.

V. CONCLUSIONS

In summary, we have developed an electronic device, based on the synchronous detection technique, for the measurement of the inverse spin Hall effect in FM/NM bilayers. The accessory was added to an ESR spectrometer and the performance was tested for different field modulation amplitudes, modulation frequencies, and microwave powers. The characterization reveals a simple method to put in phase the signal with the reference. For the modulation amplitudes and microwave powers used in the experiments, the maximum signal to noise ratio was achieved for a modulation frequency between 6 and 12 kHz. Additionally, the simplicity of the circuit can be easily adapted to measure different properties in other experiments, for example, a similar circuit can be used to measure magnetic fields by replacing the sample by a Hall probe.

ACKNOWLEDGMENTS

This work was supported in part by ANPCyT Grant Nos. PICT 2013-2363 and PICT 2013-0401, Conicet Grant No. PIP 112-201101-00482, and U. N. Cuyo Grant No. 06/C421, all from Argentina.

[1]M. Johnson and R. H. Silsbee, Phys. Rev. Lett. **55**, 1790 (1985); T. Valet and A. Fert, Phys. Rev. B **48**, 7099 (1993).
[2]Y. Tserkovnyak, A. Brataas, and G. E. W. Bauer, Phys. Rev. Lett. **88**, 117601 (2002).
[3]E. Saitoh, M. Ueda, H. Miyajima, and G. Tatara, Appl. Phys. Lett. **88**, 18 (2006).
[4]J. E. Hirsch, Phys. Rev. Lett. **83**, 1834 (1999).
[5]M. Dyakonov and V. Perel, JETP Lett. **13**, 467 (1971).
[6]C. Vittoria, *Microwave Properties of Magnetic Films* (World Scientific, Singapore, 1993).
[7]C. Vittoria, *Microwave Properties of Magnetic Films* (World Scientific, Singapore, 1993), p. 113.
[8]O. Mosendz, J. E. Pearson, F. Y. Fradin, G. E. W. Bauer, S. D. Bader, and A. Hoffmann, Phys. Rev. Lett. **104**, 046601 (2010).
[9]C. Hahn, G. de Loubens, O. Klein, M. Viret *et al.*, Phys. Rev. B **87**, 174417 (2013).
[10]A. Brataas, Y. Tserkovnyak, G. E. W. Bauer, and B. I. Halperin, Phys. Rev. B **66**, 060404(R) (2002).
[11]H. J. Jiao and G. E. W. Bauer, Phys. Rev. Lett. **110**, 217602 (2013).
[12]J. E. Gómez, B. Zerai Tedlla, N. R. Álvarez, G. Alejandro, E. Goovaerts, and A. Butera, Phys. Rev. B **90**, 184401 (2014).
[13]K. Ando, S. Takahashi, J. Ieda, Y. Kajiwara *et al.*, J. Appl. Phys. **109**, 103913 (2011).
[14]N. P. Albaugh, The Instrumentation Amplifier Handbook: Including Application, Burr- Brown Corporation, Tucson, Arizona, 2000, p. 62.
[15]C. P. Poole, Jr., *Electron Spin Resonance: A Comprehensive Treatise on Experimental Techniques*, 2th ed. (John Wiley and Sons, Inc., 1983), p. 166.